

THE PHOTOLYSIS OF METHYL GLYOXAL VAPOUR AT 436 nm

E. KYLE and S. W. ORCHARD*

Department of Chemistry, University of Natal, Pietermaritzburg (South Africa)

(Received December 30, 1976)

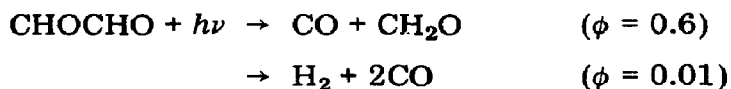
Summary

Methyl glyoxal (MG) has been photolysed in the gas phase by light of 436 nm under a variety of conditions of temperature, pressure and absorbed light intensity. Products detected were carbon monoxide, methane, ethane, acetaldehyde, acetone and biacetyl. A mechanism is proposed which qualitatively accounts for the main features of the experimental results, the two primary photochemical processes being production of carbon monoxide and a split into radicals. At 352.9 K the quantum yields for these reactions are 0.77 and 0.18, respectively. Arrhenius rate parameters for a secondary process, H atom abstraction from MG by methyl radicals, are $A = 10^{-12.64 \pm 0.38} \text{ cm}^3 \text{ molecule}^{-1} \text{ s}^{-1}$ and $E_a = 27.7 \pm 2.8 \text{ kJ mol}^{-1}$.

Introduction

The photochemistry of a number of α -dicarbonyl compounds has previously been studied, and in particular the gas phase photolyses of two of the simplest compounds, glyoxal (ethanedial) and biacetyl (2,3-butanedione), have been thoroughly investigated and reviewed [1 - 6]. Methyl glyoxal (MG) (2-oxopropanal), though intermediate in structure between glyoxal and biacetyl, has received a minimum of attention [7, 8]. However, a recent paper [9] has provided information on primary quantum yields in the photolysis of MG and has prompted this report.

When glyoxal vapour is irradiated in the first absorption band at 436 nm the main decomposition pathways are



Radical formation only occurs upon irradiation in the second band at wave-

*Present address: Department of Chemistry, University of the Witwatersrand, Johannesburg 2001, South Africa.

lengths shorter than 254 nm [10]. In contrast, the photodecomposition of biacetyl vapour at 436 nm occurs largely via the formation of acetyl and methyl radicals. At low temperatures the primary split involves a collision between two electronically excited molecules, while above 370 K the primary decomposition is first order with respect to excited molecules. Various products are then formed by the reactions of methyl radicals with biacetyl and by radical recombination reactions.

In view of the marked contrast between the photodecomposition mechanisms for glyoxal and biacetyl, there is a clear need for data on the photolysis of MG. Kirkbride and Norrish [7] obtained a large percentage of carbon monoxide among the volatile products together with a solid when they irradiated MG using an unfiltered mercury lamp. Gibson [8] photolysed MG vapour at 436 nm and 386 K, and detected carbon monoxide, methane, ethane, acetaldehyde (ethanal) and acetone (2-propanone) as products. A free radical chain mechanism was proposed to account for his findings. In this paper we present results on the photolysis of MG at 436 nm over a range of temperatures, light intensities and pressures of both MG and added gases.

Experimental

Photolyses

A cylindrical quartz photolysis cell (29 mm i.d. \times 80 mm long) with optically flat end windows was fitted with a greaseless stopcock (Springham) and housed in a well-insulated aluminium block oven. The light source was an Osram HBO 500 high pressure mercury-xenon point source arc, and the optical train was similar to that described by Calvert and Pitts [10, p. 763]. The recommended chemical filters for 436 nm were used [10, p. 737] except that the molarity of the NH_4OH was increased to 2.9 in order to avoid precipitation occurring from the $\text{CuSO}_4\text{-NH}_4\text{OH}$ solution in use. Neutral density filters, made from uniformly exposed photographic plates, were used to control the light intensity reaching the photolysis cell. The light intensity at the rear window of the cell was monitored with an RCA 935 vacuum phototube, calibrated against a 0.15 M potassium ferrioxalate actinometer [11]. Since the diameter of the light beam was slightly less than that of the cell the "light volume" was taken to be 45.8 cm^3 , corresponding to a 27 mm diameter beam.

Gas handling

The conventional high vacuum manifold used a spiral gauge for the measurement of MG pressure. After photolysis the products not condensed at 77 K (CO , CH_4) were transferred via a Toepler pump to an injection loop for gas chromatographic analysis. The condensable products were retained in a trap at 77 K during this process and were subsequently warmed and transferred to the loop for separate analysis.

Analyses

The products of the reaction were analysed by gas chromatography. The non-condensables were separated on a 2 m long stainless steel column of 6 mm diameter, packed with 30-60 mesh 5A molecular sieve. The condensable products were separated on a 3 m long column containing 60-80 mesh Chromport XXX coated with 10% Carbowax 20M. The columns were installed in a Beckman GC-M dual column gas chromatograph fitted with both a thermal conductivity detector and a flame ionisation detector, the column temperature being 333 K.

Methyl glyoxal

A 25% aqueous solution of MG (Cambrian Chemicals) was freeze dried for 12 - 15 h. The moist residue was then heated under vacuum at 380 K, generating MG which was dried by repeated vacuum distillations through a tube containing phosphoric oxide. Fractional distillation under vacuum and pumping at 195 K was used to purify further the product to about 99.5% purity. The residual acetaldehyde, acetone and biacetyl impurities were measured from time to time, and appropriate corrections were made to the analyses of photolysis product mixtures.

Gases

Argon (Afrox), high purity nitrogen (Afrox) and C.P. nitric oxide (Matheson) were used without further purification.

Results

The extinction coefficient of MG vapour at a wavelength of 436 nm and a temperature of 387 K was found to be $23 \text{ l mol}^{-1} \text{ cm}^{-1}$. In view of the broad filter bandpass and the structure in the MG absorption spectrum in this region, this value should be treated as a rough guide only.

Product quantum yields were found to be dependent on temperature, light intensity, MG concentration and pressure of added gas. A selection of results is presented below, fuller results being available elsewhere [12]. Tables 1 and 2 present the intensity dependence of quantum yields at various temperatures and concentrations of MG. The calculated quantum yields of acetone and biacetyl show considerable scatter owing to the large impurity corrections required and, in the case of biacetyl, to interference in its analysis from MG.

The temperature dependence of quantum yields is perhaps most clearly illustrated graphically. This is done in Fig. 1. The dependence of quantum yields on pressure of added nitrogen is shown in Fig. 2. Added argon had a very similar effect to nitrogen, while in one experiment at 413 K where 110 Torr (14.7 kPa) of NO was added all the usual products were almost entirely suppressed, The major "normal" product then was carbon monoxide, with a quantum yield of only 0.12.

TABLE 1
Dependence of quantum yields ϕ on absorbed light intensity at different temperatures^a

T(K)	$10^{-15} \times I_a$ (quanta s ⁻¹)	Product quantum yields					
		$10^2 \times \phi(\text{CH}_4)$	$\phi(\text{CO})$	$10^2 \times \phi(\text{C}_2\text{H}_6)$	$10 \times \phi(\text{CH}_3\text{CHO})$	$10^2 \times \phi(\text{CH}_3\text{COCH}_3)$	$10^2 \times \phi(\text{CH}_3\text{CO})_2$
352.9	20.4	0.61	0.96	0.46	0.375	1.8	7.6
352.9	12.0	0.69	0.94	0.46	0.83	2.8	4.5
352.9	6.41	1.07	1.08	0.69	1.26	3.8	4.3
352.9	2.76	1.76	1.21	1.07	1.90	4.1	5.3
352.9	0.818	4.4	1.52	1.53	4.5	5.0	5.9
412.3	32.4	12.7	1.44	9.9	3.75	3.8	0.0
412.3	18.7	11.5	2.22	12.0	4.5	5.7	0.0
412.3	11.3	15.3	2.51	13.1	5.6	4.7	0.0
412.3	6.47	15.0	2.79	19.8	9.7	5.4	0.0
412.3	2.85	16.1	3.36	25.6	20.1	10.2	0.0
412.3	0.754	38.6	5.0	29.7	24.3	9.7	0.0

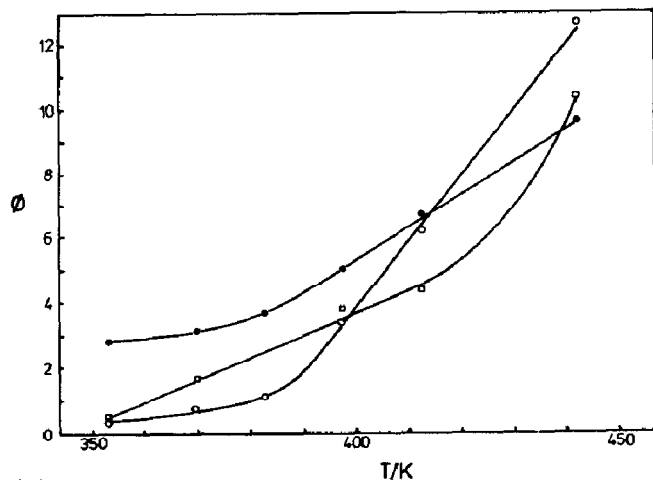
^a[MG] = $6.44 \pm 0.12 \times 10^{17}$ molecule cm⁻³. Fraction of light absorbed $I_a/I_0 = 0.38 \pm 0.01$.
See Table 2 for results at 386.7 K.

TABLE 2

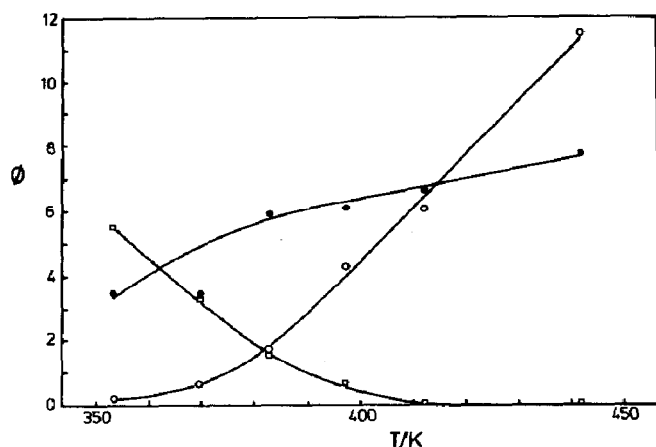
Dependence of quantum yields ϕ on absorbed light intensity I_a at different concentrations of methyl glyoxal^a

$10^{-15} \times I_a$ (quanta s^{-1})	Product quantum yields					
	$10^2 \times \phi(\text{CH}_4)$	$\phi(\text{CO})$	$10^2 \times \phi(\text{C}_2\text{H}_6)$	$10 \times \phi(\text{CH}_3\text{CHO})$	$10^2 \times \phi(\text{CH}_3\text{COCH}_3)$	$10^2 \times \phi(\text{CH}_3\text{CO})_2$
(a) $[\text{MG}] = 3.01 \pm 0.06 \times 10^{17}$ molecule cm^{-3} ; $I_a/I_0 = 0.196 \pm 0.004$						
19.0	2.95	1.12	2.19	0.87	4.5	4.5
11.2	3.48	1.23	3.03	1.26	5.3	4.8
6.75	5.3	1.27	3.18	1.45	5.2	5.2
3.41	6.2	1.49	4.6	2.42	5.5	4.7
1.36	13.5	1.90	5.0	4.1	7.3	3.3
0.409	19.7	2.79	6.8	8.7	7.3	6.7
(b) $[\text{MG}] = 6.44 \pm 0.12 \times 10^{17}$ molecule cm^{-3} ; $I_a/I_0 = 0.374 \pm 0.017$						
36.5	5.5	1.23	4.0	2.12	6.1	2.9
21.2	7.7	1.46	5.4	3.87	7.7	3.6
11.8	8.5	1.79	7.7	5.0	8.4	0.8
7.01	9.6	2.06	10.3	7.1	8.4	1.3
2.83	25.7	2.57	10.7	10.1	9.2	2.1
0.780	24.6	3.13	12.3	16.6	5.8	2.1
(c) $[\text{MG}] = 12.47 \pm 0.12 \times 10^{17}$ molecule cm^{-3} ; $I_a/I_0 = 0.598 \pm 0.007$						
53.9	6.1	1.73	7.6	3.69	11.0	3.0
32.1	7.0	1.93	8.4	5.4	6.1	4.6
18.3	7.8	2.29	12.4	8.3	10.2	7.9
10.6	8.0	2.35	13.7	9.4	7.9	5.1
4.37	14.9	3.19	12.8	11.4	5.1	7.0
1.29	20.4	3.98	24.4	26.4	4.7	8.7

^a $T = 386.7$ K.



(a)



(b)

Fig. 1. The dependence of product quantum yields on temperature ($[MG] = 6.44 \times 10^{17}$ molecule cm^{-3} , $I_a = 1.9 \times 10^{16}$ quanta s^{-1}): (a) \circ CH_4 ($\times 50$), \bullet CO ($\times 3$), \square CH_3CHO ($\times 10$); (b) \circ C_2H_6 ($\times 50$), \bullet CH_3COCH_3 ($\times 100$), \square $\text{CH}_3\text{COCOCH}_3$ ($\times 100$).

Discussion

Electronic states

Coveleskie and Yardley [9] have published the visible absorption spectrum of MG vapour, as well as the fluorescence and phosphorescence spectra of MG excited at about 440 nm. The absorption is an $\pi^* \leftarrow n$ transition occurring in the region 460 - 350 nm and shows some structure in the 430 - 460 nm region. The 0-0 band was assigned to be at either $22\,260\text{ cm}^{-1}$ (266.5 kJ mol^{-1}) or $22\,090\text{ cm}^{-1}$ (264.5 kJ mol^{-1}). The luminescence spectra indicated a triplet state about 2400 cm^{-1} below the excited singlet, putting the triplet at about 237 kJ mol^{-1} above the ground state. The 435.8 nm

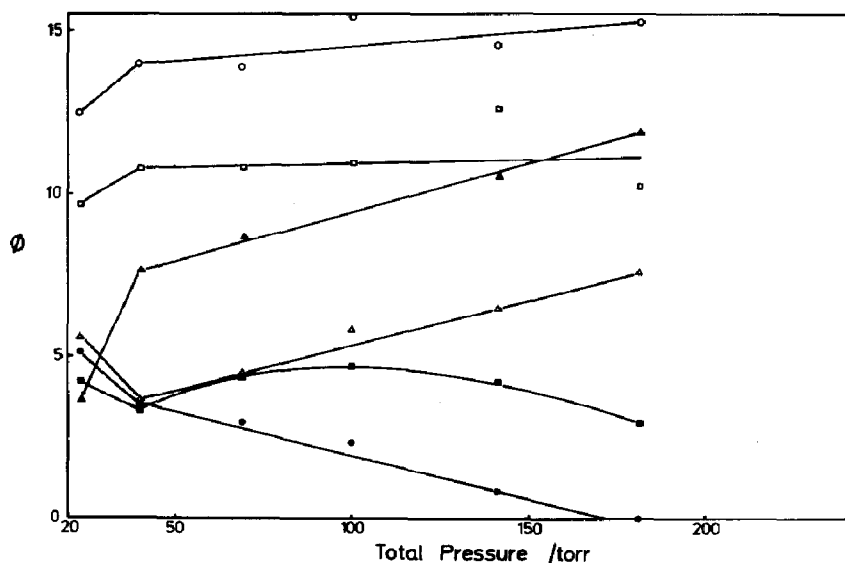


Fig. 2. The dependence of product quantum yields on added nitrogen at 352.9 K ($P_{MG} = 23.5$ Torr, 1 Torr \approx 133 Pa): \circ CO($\times 10$), \triangle C₂H₆($\times 500$), \square CH₃CHO($\times 50$), \bullet CH₃COCOCH₃($\times 100$), \blacktriangle CH₄($\times 200$), \blacksquare CH₃COCH₃($\times 100$).

(274.7 kJ mol⁻¹) photons employed in the present study would therefore produce excited singlet MG molecules with roughly 10 kJ mol⁻¹ or less of vibrational excitation.

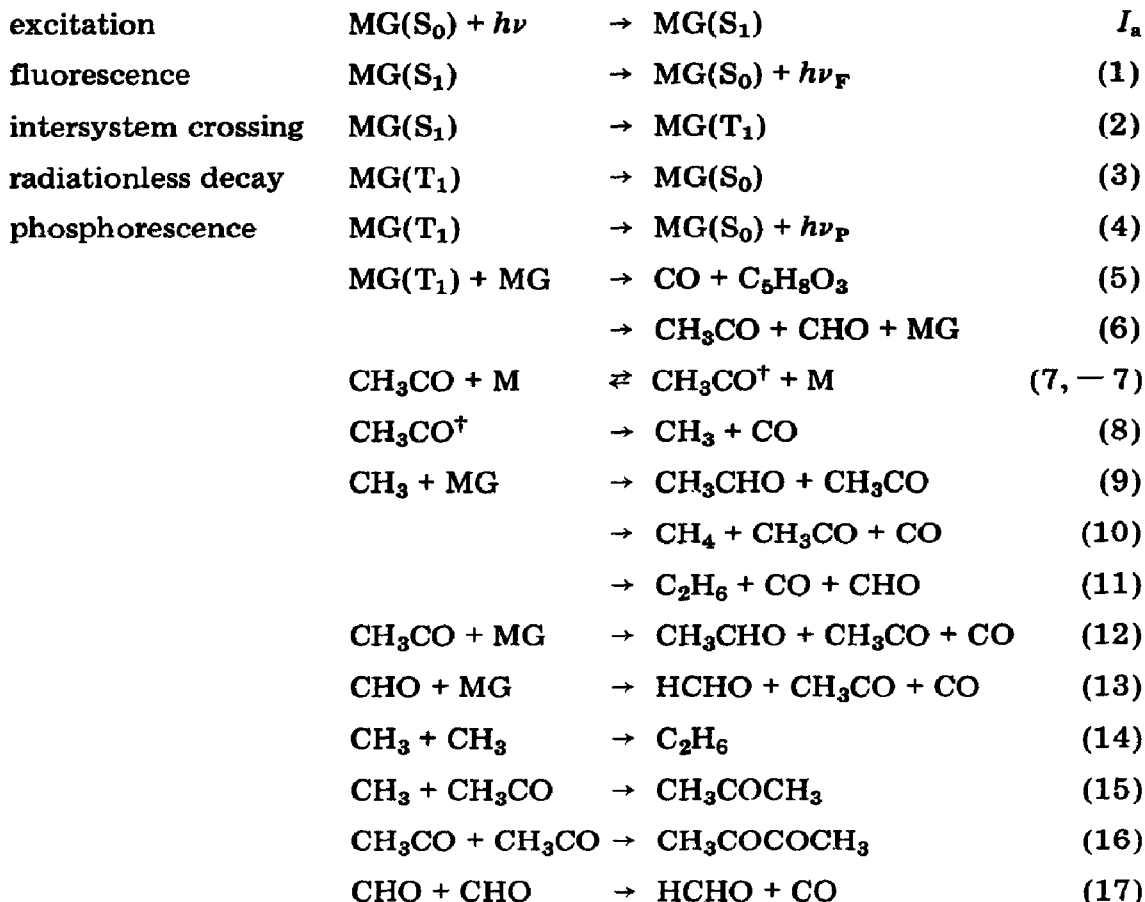
CO—CO bond energy

The energy of the CO—CO bond, the weakest in MG, may be calculated from ΔH_f° data for MG (gas), CH₃CO and CHO. The standard enthalpy of formation of MG is calculated to be -274 kJ mol⁻¹ using the enthalpy of combustion measured by Moulds and Riley [13] and an estimated value of 35 kJ mol⁻¹ for ΔH_v° at 298 K. The value of ΔH_f° for CH₃CO was taken to be -19 kJ mol⁻¹ (the average of five similar recent determinations [14]), while for CHO the recently recommended value of 42 kJ mol⁻¹ was employed [15]. On this basis the CO—CO bond energy in MG is calculated to be 297 kJ mol⁻¹. The use of Benson's "additivity" estimates [16] yields a bond energy of 311 kJ mol⁻¹, but apart from this discrepancy there is still some uncertainty about the values of ΔH_f° for the radicals, especially CHO. The bond dissociation energy, however, is almost certainly greater than the energy of a 436 nm photon, so that light-activated MG molecules probably lack sufficient energy to dissociate in the absence of collisions.

Mechanism

The marked dependence of the quantum yields of CH₄, CO, C₂H₆ and CH₃CHO on temperature and light intensity, together with the large quantum yields of CO and CH₃CHO are indicative of a free radical chain process for the photodecomposition of MG. The photodecomposition of biacetyl is known to proceed via a radical chain mechanism [2], and it is to be expected

that there will be some similarities between the two systems. Gibson [8] has studied the photolyses of MG and has proposed a mechanism involving chain propagation by formyl and acetyl radicals. The present work has covered a wider range of experimental variables than did Gibson's, and as a result additional features have emerged which suggest that Gibson's mechanism is not entirely correct. The following mechanism is now proposed to account for the photodecomposition:



Here $\text{MG}(\text{S}_0)$ and MG represent ground singlet state molecules of MG, while $\text{MG}(\text{S}_1)$ and $\text{MG}(\text{T}_1)$ represent molecules in the first excited singlet and triplet states respectively; $\text{CH}_3\text{CO}^\dagger$ represents an acetyl radical with sufficient vibrational energy to dissociate in reaction (8).

Primary decomposition

The work of Coveleskie and Yardley [9] has provided quantitative data on the relative importance of the photophysical processes following excitation of MG by 449 nm radiation. Intersystem crossing is very much faster than fluorescence ($k_1 \approx 10^5 \text{ s}^{-1}$ and $k_1 + k_2 = 4.9 \times 10^7 \text{ s}^{-1}$), while for moderate pressures self-quenching of $\text{MG}(\text{T}_1)$ (*i.e.* processes such as (5) and (6)) is

much faster than phosphorescence and radiationless decay: $(k_5 + k_6) / (k_3 + k_4) = 3.0 \text{ Torr}^{-1}$. Under the conditions employed in the present study, using a similar but not identical excitation wavelength, it can be deduced that more than about 94% of the excited MG molecules will be removed by self-quenching processes such as (5) and (6).

Our chemical results also contain information bearing on the importance of the primary chemical decomposition of reagent molecules. Examination of the results at 352.9 K reveals that carbon monoxide has a far higher quantum yield than that of all the other products combined, and that the relative discrepancy is greatest at high absorbed light intensities. In the limit of infinitely high absorbed intensity the only products formed would be those produced by the primary decomposition of light-activated reagent and those formed by radical recombination. On the basis of the proposed mechanism and assuming that at high intensities reaction (13) is unimportant in comparison with (17) for removal of CHO, the high intensity limiting value of $\phi(\text{CO})$ is equal to $\phi_5 + 0.5 \phi_6$. A plot of selected quantum yields against reciprocal absorbed light intensity is shown in Fig. 3. Some of the plots appear to be reasonably linear for low values of $1/I_a$, though at the higher temperatures the plots generally exhibit curvature over the entire intensity range. The validity of such extrapolations is therefore open to question, but it does appear that $\phi(\text{CH}_3\text{CHO})$ falls to near zero at infinite I_a , while $\phi(\text{CO})$ approaches a value slightly less than unity, *i.e.* $\phi_5 + 0.5 \phi_6 \lesssim 1$.

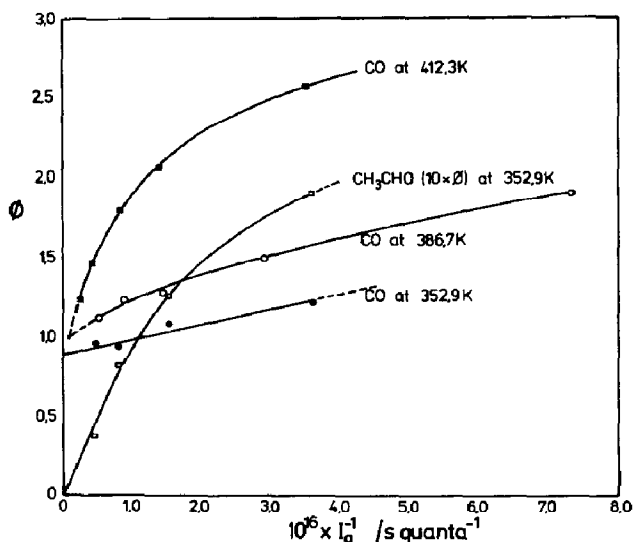


Fig. 3. A plot of the quantum yields against reciprocal absorbed light intensity.

A method of determining the value of ϕ_5 is to correct the experimental value of $\phi(\text{CO})$ for the yield of CO associated with the formation of the other measured products. This approach also depends to some extent on the assum-

ed mechanism and on accurate analyses for most products. The following relation can be derived from the proposed mechanism:

$$\phi_5 = \phi(\text{CO}) - \{ \phi(\text{CH}_3\text{CHO}) + 2\phi(\text{CH}_4) + 2\phi(\text{CH}_3\text{COCH}_3) + 3\phi(\text{C}_2\text{H}_6) + \phi(\text{CH}_3\text{COCOCH}_3) \} \quad (18)$$

The terms in braces is smaller than $\phi(\text{CO})$ and the calculated value of ϕ_5 is therefore expected to be most reliable for high values of I_a and low values of [MG]. Calculated values of ϕ_5 averaged over a wide range of I_a are presented in Table 3. Clearly a value for ϕ_5 of about 0.8 is appropriate, which is independent of temperature, pressure and light intensity, and this agrees well with the upper limit of about 1 obtained by the extrapolation procedure. Since CO is such a dominant product at high I_a , the formation of an undetected byproduct must be postulated. For this reason the unidentified high-boiling compound of formula $\text{C}_5\text{H}_8\text{O}_3$ is proposed, and this corresponds to the product identified by Kirkbride and Norrish [7] as the dimethyl derivative of glycerosone (hydroxymethyl glyoxal).

TABLE 3

Mean values of ϕ_5 and ϕ_6 obtained under various conditions of temperature and reactant pressure

P_{MG} (Torr)	T (K)	ϕ_5	Number of determinations	ϕ_6
24	352.9	0.77 ± 0.02	5	0.18 ± 0.03
12	386.7	0.86 ± 0.13	6	0.30 ± 0.06
26	386.7	0.60 ± 0.09	6	0.30 ± 0.06
50	386.7	0.76 ± 0.47	6	0.41 ± 0.04
28	412.3	0.73 ± 0.40	6	0.32 ± 0.06

At high I_a and low temperature $\phi(\text{CH}_3\text{COCH}_3) + \phi(\text{CH}_3\text{COCOCH}_3) \gg \phi(\text{C}_2\text{H}_6)$, suggesting that the radical initiation process is a reaction producing CH_3CO . A primary decomposition such as (6), in which the weakest bond in the molecule is broken, is most likely, but we cannot exclude the possibility that some CH_3 radicals are formed in a primary process (*e.g.* (6a)) as happens in the case of biacetyl photolysis [10, pp. 421 - 422].



The value of ϕ_6 can be derived from our results. At sufficiently high I_a reactions (11) and (13) may be disregarded in comparison with reactions (14) and (17) respectively:

$$\phi_6 = 2\{ \phi(\text{C}_2\text{H}_6) + \phi(\text{CH}_3\text{COCH}_3) + \phi(\text{CH}_3\text{COCOCH}_3) \} \quad (19)$$

Values of ϕ_6 calculated from (19) using data from high light intensity experiments are listed in Table 3. There appears to be an increase in the calculated

ϕ_6 with increasing pressure and temperature, and the temperature effect is confirmed when a wider range of temperatures is considered (*e.g.* the use of data contained in Fig. 1). Radical recombination reactions have small or zero activation energies and are thus favoured over chain propagation reactions at low temperature. We therefore consider the "best" value for ϕ_6 to be that at 352.9 K, where $\phi_6 = 0.18 \pm 0.03$. If reaction (17) is replaced by (13), as may occur at higher temperatures, eqn. (19) must be replaced by

$$\phi_6 = \phi(\text{C}_2\text{H}_6) + \phi(\text{CH}_3\text{COCH}_3) + \phi(\text{CH}_3\text{COCOCH}_3) \quad (20)$$

This explains why ϕ_6 as calculated from (19) apparently increases with temperature.

Using the "best" values for ϕ_5 and ϕ_6 (from data obtained at 352.9 K) we obtain $\phi_5 + \phi_6 = 0.95 \pm 0.04$, in excellent agreement with the self-quenching quantum yield of greater than about 0.94 deduced from luminescence measurements [9]. Clearly any self-quenching reactions other than (5) and (6) and/or (6a) must be of very minor importance.

Secondary reactions

The reasons for invoking the chain propagation and termination reactions (7) - (17) will be briefly set out. The quasi-unimolecular decomposition of acetyl radicals (reactions (7), (-7) and (8)) is well known [17] and there is good evidence for these reactions in the decrease of $\phi(\text{CH}_3\text{COCOCH}_3)$ with increasing temperature and pressure of added nitrogen (Figs. 1 and 2). The recombination and disproportionation reactions (14) - (17) are also well documented [2, 14, 18].

Quantum yields with a strong inverse intensity dependence are indicative of products formed in chain propagating steps. The quantum yield of C_2H_6 shows an inverse dependence on I_a , and a chain propagation step such as (11) must therefore be operative in addition to the termination step (14). The high $\phi(\text{C}_2\text{H}_6)$ values at elevated temperatures are also consistent with this argument. The quantum yield of CH_3CHO shows less temperature dependence than $\phi(\text{CH}_4)$ and less dependence on added N_2 . Reactions (9) and (10) alone cannot account for this, so reaction (12) has been included as a second acetaldehyde-producing process which should be important at low temperature and low additive pressure.

The fate of CHO poses a problem in that no products uniquely attributable to these radicals were detected. Reactions (13) and (17) both produce formaldehyde which would not normally be detected by gas chromatography.

Some quantitative data on the secondary reactions may be deduced. At high intensities (11) may be ignored in comparison with (14) for the production of ethane. We can then obtain the relation

$$[\text{CH}_3]_{\text{ss}} = \left\{ \frac{R(\text{C}_2\text{H}_6)}{k_{14}} \right\}^{1/2} = \frac{R(\text{CH}_4)}{k_{10}[\text{MG}]}$$

where R_i is the rate of production of i per unit volume and $[\text{CH}_3]_{\text{ss}}$ is the steady state concentration of CH_3 radicals. We define F as

$$F = \frac{\{R(\text{C}_2\text{H}_6)\}^{1/2}}{R(\text{CH}_4)} = \frac{\{(I_a/V)\phi(\text{C}_2\text{H}_6)\}^{1/2}}{(I_a/V)\phi(\text{CH}_4)} = \frac{k_{14}^{1/2}}{k_{10}[\text{MG}]} \quad (21)$$

where V is the "light volume" of the cell which is 45.8 cm^3 . Values of F were calculated from quantum yield data at temperatures in the range $352.9 - 442.0 \text{ K}$ for $[\text{MG}] = 6.44 \times 10^{17} \text{ molecule cm}^{-3}$ and $I_a = 1.90 \times 10^{16} \text{ quanta s}^{-1}$. A plot of $-\ln F$ against $1/T$ showed scatter but no apparent non-linearity (Fig. 4). If k_{14} is known, the slope and intercept of this plot with the $\ln F$ axis yield the Arrhenius parameters for k_{10} . A temperature-independent value of $k_{14} = 5.3 \times 10^{-11} \text{ cm}^3 \text{ molecule}^{-1} \text{ s}^{-1}$, the average of a number of recent measurements [19], was assumed. Then $A_{10} = 10^{-12.64 \pm 0.38} \text{ cm}^3 \text{ molecule}^{-1} \text{ s}^{-1}$ and $E_{10} = 27.7 \pm 2.8 \text{ kJ mol}^{-1}$ (errors are standard deviations). These parameters are very similar to those for aldehydic H atom abstraction by CH_3 from CH_3CHO [20] ($A = 10^{-12.28} \text{ cm}^3 \text{ molecule}^{-1} \text{ s}^{-1}$ and $E_a = 28.5 \text{ kJ mol}^{-1}$).

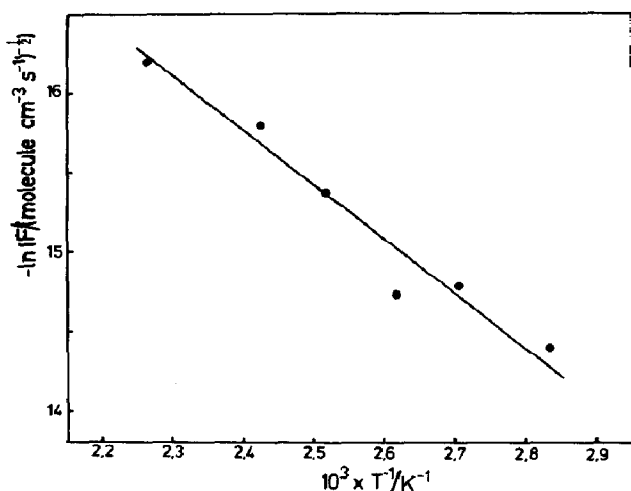


Fig. 4. A plot of $-\ln F$ against reciprocal temperature, where $F = \{R(\text{C}_2\text{H}_6)\}^{1/2} / R(\text{CH}_4)$.

As a consequence of the numerous secondary reactions occurring in this system it is difficult to extract much additional quantitative data on rate constants from our results. The expressions for the dependence of individual product quantum yields on experimental variables are rather complex and there is little to be gained from attempts to relate experimental results to the mechanistic predictions in this way. For the study of the secondary reactions occurring in this system, alternative methods would generally be more fruitful.

Arguments can be advanced for the inclusion of a number of reactions other than those proposed in the mechanism. Such reactions include



Reactions (22) and (23) have been postulated to occur in related gas phase systems [18] (acetaldehyde pyrolysis and photolysis), while (24) could account for the apparent slight intensity dependence of $\phi(\text{CH}_3\text{COCH}_3)$ under some conditions. However, these reactions are at best likely to be of minor importance and will have only a small effect on the calculated values of ϕ_5 , ϕ_6 and k_{10} .

In conclusion the primary photochemical processes occurring in MG vapour are substantially different from those occurring in the related α -dicarbonyls, glyoxal and biacetyl. In common with biacetyl a number of products are formed in a secondary radical chain mechanism. The primary quantum yields are $\phi_5 = 0.77$ and $\phi_6 = 0.18$ at 352.9 K.

Acknowledgment

We thank the C.S.I.R. for financial assistance.

References

- 1 C. S. Parmenter, *J. Chem. Phys.*, 41 (1964) 658.
- 2 F. E. Blacet and W. E. Bell, *Disc. Faraday Soc.*, 14 (1953) 70, 131.
- 3 W. A. Noyes, W. A. Mulac and M. S. Matheson, *J. Chem. Phys.*, 36 (1962) 880.
- 4 R. B. Cundall and A. S. Davies, in G. Porter (ed.), *Progress in Reaction Kinetics*, Vol. 4, Pergamon Press, Oxford, 1967, pp. 178 - 184.
- 5 J. N. Pitts Jr. and J. K. S. Wan, in S. Patai (ed.), *The Chemistry of the Carbonyl Group*, Wiley-Interscience, New York, 1966, pp. 871 - 873.
- 6 B. M. Monroe, in J. N. Pitts Jr., G. S. Hammond and W. A. Noyes Jr. (eds.), *Advances in Photochemistry*, Vol. 8, Wiley-Interscience, New York, 1971, pp. 80 - 85.
- 7 F. W. Kirkbride and R. G. W. Norrish, *Trans. Faraday Soc.*, 27 (1931) 404.
- 8 B. A. St. C. Gibson, M.Sc. Thesis, University of Natal, South Africa, 1968.
- 9 R. A. Coveleskie and J. T. Yardley, *J. Am. Chem. Soc.*, 97 (1975) 1667.
- 10 J. G. Calvert and J. N. Pitts Jr., *Photochemistry*, Wiley-Interscience, New York, 1966.
- 11 C. G. Hatchard and C. A. Parker, *Proc. R. Soc. London, Ser. A*, 235 (1956) 518.
- 12 S. W. Orchard, M. Sc. Thesis, University of Natal, South Africa, 1969.
- 13 L. de V. Moulds and H. L. Riley, *J. Chem. Soc., Part I* (1938) 621.
- 14 K. W. Watkins and W. W. Word, *Int. J. Chem. Kinet.*, 6 (1974) 855.
- 15 P. Warneck, *Z. Naturforsch., Teil A*, 29 (1974) 350.
- 16 S. W. Benson, *Thermochemical Kinetics*, Wiley-Interscience, New York, 1968, Chap. 2.
- 17 H. E. O'Neal and S. W. Benson, *J. Chem. Phys.*, 36 (1962) 2196.
- 18 E. W. R. Steacie, *Free Radical Mechanisms*, Reinhold, New York, 1946, Chaps. 3, 5.
- 19 F. C. James and J. P. Simons, *Int. J. Chem. Kinet.*, 6 (1974) 887.
- 20 J. A. Kerr, in C. H. Bamford and C. F. H. Tipper (eds.), *Comprehensive Chemical Kinetics*, Vol. 18, Elsevier, Amsterdam, 1976, p. 61.